

pubs.acs.org/joc Article

Role of Steric Effects on Rates of Hydrogen Atom Transfer Reactions

Yi Sun, Fengjiao Liu, Jacob N. Sanders, and K. N. Houk*



Cite This: J. Org. Chem. 2023, 88, 12668-12676



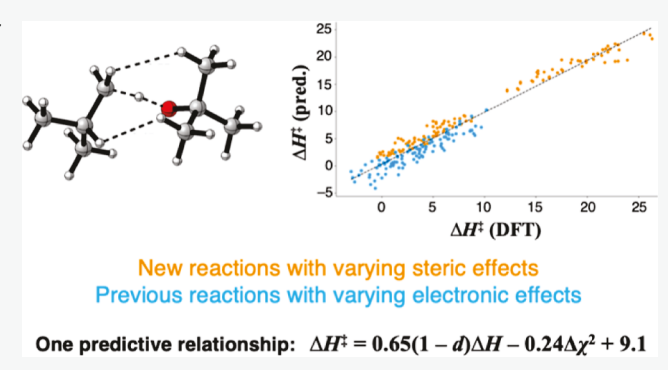
ACCESS

III Metrics & More

Article Recommendations

Supporting Information

ABSTRACT: The influence of steric effects on the rates of hydrogen atom transfer (HAT) reactions between oxyradicals and alkanes is explored computationally. Quantum chemical density functional theory computations of transition states show that activation barriers and reaction enthalpies are both influenced by bulky substituents on the radical but very little by substituents on the alkane. The activation barriers remain roughly correlated with reaction enthalpies via the Evans—Polanyi relationship even when steric repulsion effects become important, although dispersion effects sometimes stabilize transition states. By making comparisons to previously developed Evans—Polanyi and modified Roberts—Steel relationships, we find that HAT reactions between bulky molecules remain well-described by these relationships.



1. INTRODUCTION

Hydrogen atom transfer (HAT) reactions are among the most fundamental chemical reactions

$$A - H + B' \rightarrow A' + B - H \tag{1}$$

These reactions are key to a wide range of chemical, environmental, and biological processes. Recently, a number of photo-induced ¹⁻³ and electrochemical ⁴ HAT reactions with value in synthetic organic chemistry have been reported, as well as numerous case studies of HAT reactions involving metal species. ⁵⁻⁸

One of the major goals of chemists who have explored these reactions is to understand selectivities and to be able to predict which hydrogen will be abstracted, leading to a newly functionalized site. In a classic case, Baran et al. developed a bulky dioxirane to oxidize a complex steroidal system selectively and, combined with computations from the Houk group, showed how steric acceleration favored reaction at one site in a hydrogen-abstraction-dominated transition state (Figure 1a). White et al. have reported selective oxidations by a nonheme iron catalyst and have used a combination of electronic, steric, and stereoelectronic factors to rationalize these selectivities (Figure 1b).¹⁰ Bietti et al. have described selective hydrogen abstractions by the cumyloxyl radical in substituted cyclohexanes (Figure 1c).11 In each of these examples, computations were used to explore the specific cases and to provide insights into the origins of selectivity. Our study now explores one additional factor that has not generally been considered, the steric hindrance or attraction that can occur between the abstracting radical and the substrate.

There have been many more general studies aimed at understanding the barrier heights and rates of HAT reactions.

A celebrated example is the Bell–Evans–Polanyi principle, ^{12,13} which can be expressed mathematically as eq 2

$$\Delta H^{\ddagger} = E_0 + \alpha \Delta H \tag{2}$$

Here, ΔH^{\ddagger} is the activation barrier of the reaction, i.e., barrier height, ΔH is the enthalpy change of the reaction, and E_0 and α are empirical fitting parameters. In particular, the parameter α is the slope of the regression line in a plot of ΔH^{\ddagger} vs ΔH and is related to the position of the transition state along the reaction coordinate. It is often around 0.5 for Evans—Polanyi correlations.

A refinement of the Bell–Evans–Polanyi principle is the Roberts–Steel relationship, which, in addition, accounts for polar and conjugation effects. Recent work by Liu et al. Serived a simplified Roberts–Steel relationship (eq 3) in which the activation barrier of the reaction, ΔH^{\ddagger} , depends on three quantities: the reaction enthalpy, ΔH ; the difference between the electronegativities, $\Delta \chi$, of the reactant and product radicals; and a quantity d whose value depends on whether the substrate has α -unsaturation present relative to the reacting C–H bond. This gives rise to the equation

$$\Delta H^{\ddagger} = \alpha (1 - d) \Delta H + \beta \Delta \chi^2 + \gamma \tag{3}$$

Received: June 19, 2023 Published: August 21, 2023





(a) Selective hydrogen abstraction by dioxiranes

(b) Selective hydrogen abstraction by non-heme iron-oxo species

Figure 1. Examples of selective hydrogen atom abstractions by (a) dioxiranes, (b) a nonheme iron-oxo species, and (c) the cumyloxyl radical.

in which α , β , and γ are empirical fitting parameters. Alternative formulas without completely empirical fitting parameters have also been advanced by Zavitsas. ¹⁶

Another strategy to understand the barriers of HAT reactions is to use the Marcus cross relationship, which was shown by Mayer¹⁷ to relate the HAT reaction barrier heights to the self-exchange rate constants and the chemical equilibrium constant of the HAT reaction via eq 4

$$k_{\rm AH/B} = \sqrt{k_{\rm AH/A}k_{\rm BH/B}K_{\rm eq}f} \tag{4}$$

In this equation, $k_{\rm AH/A}$ and $k_{\rm BH/B}$ are the rate constants for the respective self-exchange HAT reactions, and $K_{\rm eq}$ is the equilibrium constant of the HAT reaction, which can be calculated from the change in the Gibbs free energy, ΔG , of the reaction; f is a dimensionless proportionality factor. Thus, Marcus theory relates HAT reaction barriers to kinetic factors, namely, the intrinsic barriers of self-exchange, and to thermodynamic factors, namely, the free energy change of the HAT reaction. By contrast, the modified Roberts—Steel relationship uses intrinsic properties of the reactants and products, namely, the electronegativities of the two radicals as well as the presence or absence of α -unsaturation relative to the reacting C—H bond, along with thermodynamic factors, namely, the enthalpies of reactions, to understand reaction barriers.

More recently, the Xin Hong group at Zhejiang University has developed machine learning models to correlate rates of HAT reactions with many different descriptors of the reactants and products. We have been carrying out parallel efforts and collaborations to understand the fundamental factors controlling rates. In this paper, we explore whether steric effects involving bulky groups on radicals or substrates have a significant influence on the rates of HAT reactions.

2. STERIC REPULSION AND ATTRACTION

Although the relationships discussed in the previous section have been used to explore many types of HAT reactions, those studies have included few sterically hindered substrates or radicals. Here, we explored whether steric factors affect the rates of HAT reactions. Bulky groups might slow HAT by increasing the energies of transition states via steric repulsion or, if atoms just touch, then dispersion interactions could accelerate the HAT reaction. ¹⁹ Such dispersion effects have been noted in a number of homolysis and radical recombination reactions but not yet in hydrogen abstraction by radicals. ¹⁹

There are many examples where steric effects influence the reactivity of molecules and the selectivity of substitution reactions;^{20–22} they can even determine whether certain radicals are stable in the first place.^{23,24} Nevertheless, systematic studies of steric effects in HAT reactions across a wide range of substrates are scarce.

In this work, we investigate the role of steric effects in HAT reactions between several alkoxy and phenoxy radicals and alkane substrates. We discover that steric effects may influence not only barrier heights but also reaction enthalpies.

3. COMPUTATIONAL METHOD

Ground and transition structures were optimized at the ω B97x-D/6-31G(d) level of theory²⁵⁻²⁸ using Gaussian 16.²⁹ Optimized structures were confirmed via frequency calculations, with ground states having all positive frequencies and transition states having one imaginary frequency corresponding to the reaction coordinate. These frequencies were also used to compute enthalpies at 298 K and a standard state of 1 atm. Energies were corrected via single-point computations performed at the ω B97x-D/6-311G++(d,p) level of theory.

Figure 2. 10 radicals studied in this work.

Liu et al. ¹⁵ conducted extensive benchmarking of HAT reactions and found that this level of theory, and the ω B97x-D functional in particular, offers excellent agreement with more expensive DLPNO-CCSD(T)/cc-pVTZ single-point computations as well as good agreement with experimental activation energies.

4. RESULTS AND DISCUSSION

We explored 120 HAT reactions between 10 radicals and 12 alkane C—H bonds. The structures of the alkoxy, phenoxy, and cyclohexoxy radicals are shown in Figure 2, while the structures of the alkane substrates are shown in Figure 3 with the reacting C—H bonds drawn explicitly. For the radicals, we studied 4 simple alkoxy radicals ranging from methoxy to *tert*-butoxy to determine whether the more crowded *tert*-butyl group would alter steric repulsion in these reactions. We also studied the cyclohexoxy radical and its tetramethyl derivative with two

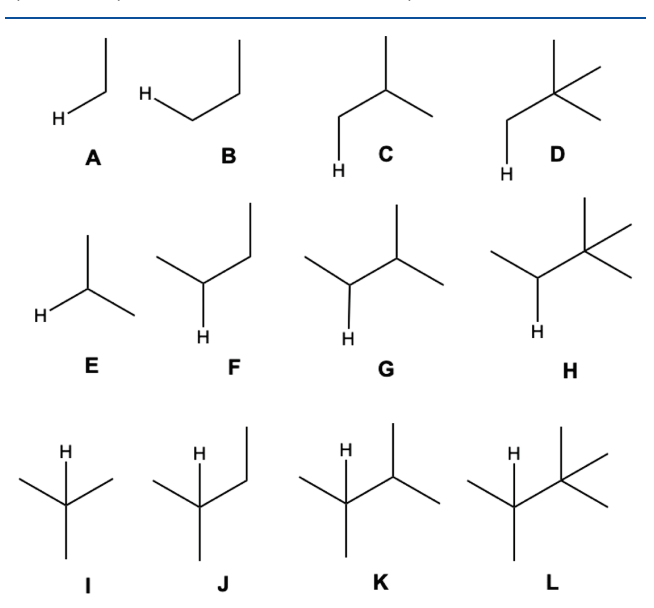


Figure 3. 12 alkane C-H bonds studied in this work with the abstracted hydrogen drawn explicitly.

adjacent quaternary carbons, the latter having a hindered environment around the oxy radical. (Although under experimental conditions, both of these cyclohexoxy radicals would undergo β -scission, ³⁰ they remain useful in computations for elucidating trends related to steric hindrance in HAT reactions.) Finally, we studied the phenoxy radical and its 2,6-dimethyl and 2,6-di-tert-butyl derivatives to assess the influence of bulky ortho substituents. The unhindered *p-tert*-butyl derivative was also included to control for electronic influence, assumed to be similar for ortho and para substituents, without an associated steric effect. No polar substituents or heteroatoms were included. All barrier heights (ΔH^{\ddagger}) are shown in Table 1, with the corresponding reaction enthalpies (ΔH) shown in Table 2.

4.1. Evans–Polanyi Relationship for Sterically Unhindered Reactions. To assess the accuracy of the Evans–Polanyi relationship for sterically unhindered reactions, we compare the reactivities of unhindered primary (A), secondary (E), and tertiary (I) C–H bonds in alkanes for three unhindered alkoxy (1), cycloalkoxy (9), and phenoxy (5) radicals. Taking differences of the Evans–Polanyi relationship for two reactions with the same E_0 and α parameters yields

$$\Delta \Delta H^{\ddagger} = \alpha \Delta \Delta H \tag{5}$$

When the two HAT reactions being compared involve the same oxy radical, then $\Delta\Delta H$ depends only on the alkane (it is the difference in bond dissociation enthalpies of the C–H bonds in the alkanes of the two reactions), whereas $\Delta\Delta H^{\ddagger}$ is different for different oxy radicals.

Table 3 shows the changes in reaction enthalpies and barrier heights in moving from sterically unhindered primary (A) to secondary (E) to tertiary (I) alkane C-H bonds for methoxy (1), cyclohexoxy (9), and phenoxy (5) radicals.

As shown in the first row of the table, the relative reaction enthalpies $\Delta\Delta H$ become more negative as the alkane C–H bond becomes more substituted because the product radical is stabilized by alkyl groups. Surprisingly, with the exception of the phenoxy radical 5, the relative barrier heights $\Delta\Delta H^{\ddagger}$ track the relative reaction enthalpies $\Delta\Delta H$ quite closely for methoxy and cyclohexoxy. This implies that α in the Evans–Polanyi relationship is approximately 1. The small (-0.6 and -0.8

Table 1. Barrier Heights (ΔH^{\ddagger}) in kcal/mol for All 120 HAT Reactions Studied in This Work

radical	1	2	3	4	5	6	7	8	9	10
alkane										
A	6.9	7.7	6.1	5.1	19.5	21.5	20.6	26.3	5.7	8.7
В	7.1	8.2	6.6	5.4	19.9	22.0	21.4	26.1	6.0	8.8
C	6.5	7.6	5.9	5.0	19.3	23.0	20.6	25.5	5.3	8.1
D	6.1	7.1	5.3	4.4	19.9	22.7	21.0	25.5	5.0	8.0
E	4.1	4.6	3.0	2.7	15.7	18.4	17.1	22.0	2.7	5.4
F	4.2	5.2	3.9	2.6	16.3	18.5	17.5	21.8	3.2	6.0
G	3.6	5.0	3.2	2.4	16.3	19.1	17.6	23.1	1.9	5.3
H	3.2	4.1	2.1	1.3	15.1	17.5	16.6	22.2	1.6	5.5
I	1.8	2.7	0.9	0.6	13.3	15.8	14.7	23.0	1.0	4.2
J	2.0	3.0	1.3	0.8	13.2	15.2	14.6	23.9	1.1	4.5
K	1.2	2.1	0.2	-0.4	12.2	15.2	13.5	21.7	-0.2	4.0
L	0.7	1.7	-0.1	-0.4	12.2	15.1	13.5	22.7	0.1	4.2

Table 2. Reaction Enthalpies (ΔH) in kcal/mol for All 120 HAT Reactions Studied in This Work

radical	1	2	3	4	5	6	7	8	9	10
alkane										
A	-0.8	-0.5	-2.1	-2.9	14.9	19.2	16.5	22.2	-1.8	-0.4
В	0.2	0.5	-1.0	-1.9	16.0	20.2	17.6	23.3	-0.8	0.7
C	0.5	1.1	-0.7	-1.6	16.3	20.5	17.9	23.6	-0.5	1.0
D	0.8	1.1	-0.5	-1.3	16.5	20.8	18.1	23.8	-0.2	1.2
E	-4.0	-3.7	-5.3	-6.1	11.7	16.0	13.3	19.0	-5.0	-3.6
F	-3.1	-2.8	-4.4	-5.2	12.6	16.9	14.2	19.9	-4.1	-2.6
G	-3.4	-2.8	-4.7	-5.5	12.3	16.6	13.9	19.6	-4.4	-3.0
Н	-3.1	-2.8	-4.3	-5.2	12.7	16.9	14.3	19.9	-4.1	-2.6
I	-6.2	-5.9	-7.5	-8.3	9.5	13.8	11.2	16.8	-7.2	-5.7
J	-5.8	-5.5	-7.1	-7.9	9.9	14.2	11.5	17.2	-6.8	-5.3
K	-6.4	-5.8	-7.7	-8.6	9.3	13.5	10.9	16.6	-7.5	-6.0
L	-6.0	-5.8	-7.3	-8.2	9.7	14.0	11.3	17.0	-7.1	-5.6

Table 3. Relative Reaction Enthalpies (Row 1) and Relative Barrier Heights (Rows 2-4) with 1 to 2 to 3° Alkanes for Hydrogen Abstractions by Radicals 1, 9, and 5 (kcal/mol)

	EtH (1°) (A)	<i>n</i> -PrH (2°) (E)	<i>i</i> -BuH (3°) (I)
$\Delta \Delta H$	0	-3.2	-5.4
methoxy (1) $\Delta \Delta H^{\ddagger}$	0	-2.8	-5.1
cyclohexoxy (9) $\Delta \Delta H^{\ddagger}$	0	-3.0	-4.7
phenoxy (5) $\Delta \Delta H^{\ddagger}$	0	-3.8	-6.2

kcal/mol) negative deviations in $\Delta\Delta H^{\ddagger}$ for the reaction between the phenoxy radical and propane and isobutane indicate that there is more stabilization in the transition state than in the product, likely due to dispersion interactions. We discuss these more later.

4.2. Electronic Effects of Alkyl Substituents on the Phenoxy Radicals in HAT Reactions. In order to study the steric effects of phenoxy radicals on the rates of HAT reactions, we first determined the electronic effect of alkyl substituents on phenoxy radical energetics. We compared the reactivities of unhindered phenoxy (5) and *p-tert*-butylphenoxy (7) radicals for a series of increasingly substituted alkanes, namely, ethane (A), propane (B), isobutane (C), and neopentane (D). Because we make comparisons between different oxy radicals with individual alkanes, $\Delta\Delta H$ depends only on the oxy radicals (it is the difference in bond dissociation enthalpies of the O–H bonds in the phenols of the two reactions), whereas $\Delta\Delta H^{\ddagger}$ is different for different alkane substrates. The results are shown in Table 4.

Table 4. Relative Reaction Enthalpies (Row 1) and Relative Barrier Heights (Rows 2–5) of Hydrogen Abstraction for Phenoxy and p- t Bu-Phenoxy Radicals (kcal/mol)

	PhO (5)	p - t BuPhO (7)
$\Delta\Delta H$	0	1.6
ethane (A) $\Delta \Delta H^{\ddagger}$	0	1.1
propane (B) $\Delta \Delta H^{\ddagger}$	0	1.5
isobutane (C) $\Delta \Delta H^{\ddagger}$	0	1.3
neopentane (D) $\Delta \Delta H^{\ddagger}$	0	1.1

Because para-substitution in 7 does not create any additional steric interactions in the HAT transition state or in the newly formed phenol O–H bond in the product, comparing the HAT reactivity of phenoxy radicals 5 and 7 shows that the p- t Bu group in 7 stabilizes the phenoxy radical starting material via hyperconjugation, thus increasing the relative enthalpies of both the transition state and the product. The reaction enthalpy (ΔH) increases by 1.6 kcal/mol, while barrier heights increase by about 1.3 kcal/mol on average, consistent with an Evans–Polanyi α of approximately 0.8.

4.3. Steric Effects of Phenoxy Radicals in HAT Reactions. Having considered the electronic effect of a *ptert*-butyl, we investigated the steric effects of phenoxy radicals on the rates of HAT reactions by considering ortho-substituted phenoxy radicals. The reactivities of increasingly hindered phenoxy (5), 2,6-dimethylphenoxy (6), and 2,6-di-*tert*-butylphenoxy (8) with ethane (A), propane (B), isobutane

(C), and neopentane (D) are summarized in Table 5. As in the previous section, $\Delta \Delta H$ is the same for any alkane substrate.

Table 5. Relative Reaction Enthalpies (Row 1) and Relative Barrier Heights (Rows 2-5) for Hydrogen Abstraction by Phenoxy and Ortho-Substituted Phenoxy Radicals (kcal/mol)

	PhO (5)	di-MePhO (6)	di- ^t BuPhO (8)
$\Delta \Delta H$	0	4.3	7.3
ethane (A) $\Delta \Delta H^{\ddagger}$	0	2.0	6.8
propane (B) $\Delta \Delta H^{\ddagger}$	0	2.1	6.2
isobutane (C) $\Delta \Delta H^{\ddagger}$	0	3.7	6.2
neopentane (D) $\Delta \Delta H^{\ddagger}$	0	2.8	5.6

The ΔH values become larger along the series 5, 6, and 8 because the Me and 'Bu groups stabilize the reactant radical relative to the product phenol. For all four alkanes, the barrier heights ΔH^{\ddagger} (the last four rows of the table) increase as the ortho-substituents become bulkier from H (5) to Me (6) to ^tBu (8) due to stabilization by the ortho alkyl groups that contribute to the increase in $\Delta\Delta H$ with ortho-substitution and the increasing steric repulsion in the transition states between these ortho-substituents and atoms of the alkane. However, surprisingly, there is an even larger increase in the reaction enthalpies even though ΔH reflects the difference in enthalpy between separated products and separated starting materials, meaning that no interaction between the ortho-substituents and the atoms of the alkane occurs. We also note a negative deviation in $\Delta \Delta H^{\ddagger}$ for the reactions of neopentane (D) with both ortho-substituted phenoxy radicals, likely due to dispersion (see later).

To understand why bulky ortho-substituents lead to higher reaction enthalpies, we first note that the electronic stabilization of 1.6 kcal/mol described in the previous section for para-substituted phenoxy radical 7 will also exist for orthosubstituted 6 and 8. Given that 6 and 8 each have two alkyl substituents, we estimate this electronic stabilization as 2×1.6 kcal/mol = 3.2 kcal/mol. However, this still leaves approximately 1.1 kcal/mol in 6 and 5.1 kcal/mol in 8 which cannot be explained by electronic effects.

To explain these remaining contributions to $\Delta\Delta H$, we identify a steric effect present in the phenol product. In particular, as the *ortho*-substituents become bulkier, i.e., from H to Me to 'Bu, the hydrogen on the phenol OH experiences more steric repulsion with ortho groups, raising the relative enthalpy of the phenol product. Figure 4 shows the shortest H–H distance between the phenol hydrogen and the nearest ortho-substituent H in the phenol products of 5, 6, and 8.

As the figure shows, the H–H bond distance decreases from 2.29 Å in phenol to 2.24 Å in 2,6-dimethylphenol to 1.83 Å in 2,6-di-*tert*-butylphenol. Given that twice the van der Waals radius of hydrogen is 2.4 Å, this represents steric repulsion between the Hs of the newly-formed O–H bond and the ortho-substituents of the product phenol. The OH always remains in the phenyl plane to maximize O lone pair—phenyl π conjugation. By this mechanism, the bulky ortho-substituents destabilize product phenols relative to the starting phenoxy radicals and thus increase the HAT reaction enthalpy ΔH . Ortho-substituents thus destabilize both the transition states and the phenol products relative to the starting materials.

This means that the Evans-Polanyi relationship between ΔH^{\ddagger} and ΔH can still hold when steric repulsions are present,

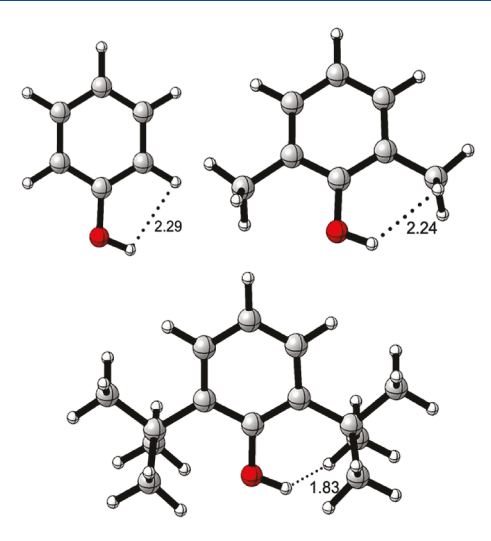


Figure 4. Shortest H–H distance (in Å) between the phenolic hydrogen and the nearest hydrogen in phenol (top), 2,6-dimethylphenol (center), and 2,6-di-*tert*-butylphenol (bottom).

as analyzed in detail in Section 4.5 below. Quantitatively, orthomethyl groups increase barrier heights by an average of 2.7 kcal/mol and reaction enthalpies by 4.3 kcal/mol, while orthotert-butyl groups increase barrier heights by an average of 6.2 kcal/mol and reaction enthalpies by 7.3 kcal/mol, leading to an Evans–Polanyi fitting parameter α in the range of 0.6–0.85, not far from the estimated value of 0.8 in the absence of steric effects.

Moving beyond phenoxy radicals, we observe a similar increase in HAT barrier heights and reaction enthalpies when comparing the cyclohexoxy radical (9) with the sterically hindered 2,2,6,6-tetramethylcyclohexoxy radical (10), as shown in Table 6 below. The steric effects of the four methyls

Table 6. Relative Reaction Enthalpies (Row 1) and Relative Barrier Heights (Rows 2-5) for Hydrogen Abstraction for Cyclohexoxy and 2,2,6,6-Tetramethylcyclohexoxy Radicals (kcal/mol)

	CyO (9)	2,2,6,6-tetra-MeCyO (10)
$\Delta \Delta H$	0	1.5
ethane (A) $\Delta \Delta H^{\ddagger}$	0	3.0
propane (B) $\Delta \Delta H^{\ddagger}$	0	2.8
isobutane (C) $\Delta \Delta H^{\ddagger}$	0	2.8
neopentane (D) $\Delta \Delta H^{\ddagger}$	0	3.0

destabilize the TS twice as much (\sim 3 kcal/mol) as they destabilize the product (\sim 1.5 kcal/mol), so there is a larger steric effect in the TS than in the product. Figure 5 shows the HH repulsions in the TSs that presumably destabilize the TS. The product destabilization is less because it is the result of the H(O) intramolecular repulsions, as in the substituted phenoxy cases.

4.4. Steric Attraction in HAT Reactions of Alkoxy Radicals and Alkanes. Next, we consider the role of steric attraction, or dispersion interactions, ¹⁹ in the barrier heights of HAT reactions. Among the alkoxy radicals in our study, the bulkiest is *tert*-butoxy radical **4**, while the least bulky is methoxy radical **1**. With these two alkoxy radicals, we can compare the most hindered and least hindered reactions in our study for primary, secondary, and tertiary alkane C–H bonds. For primary alkane C–H bonds, the least hindered HAT

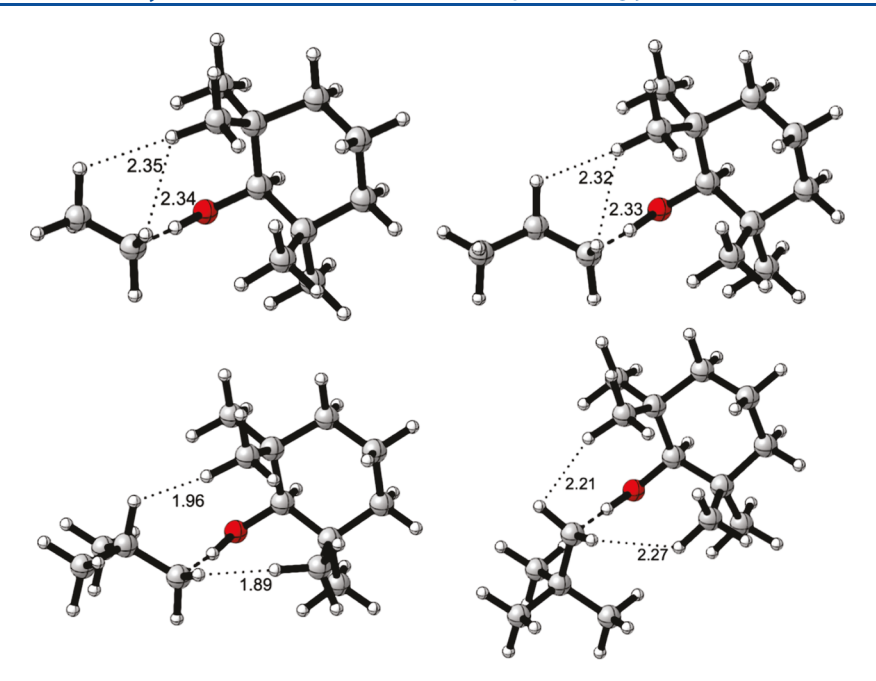


Figure 5. Transition states for HAT by the tetramethylcyclohexoxy radical from ethane (A) (upper left), propane (B) (upper right), isobutane (C) (lower left), and neopentane (D) (lower right). The nonbonding distances shown are the approaches of radical and alkane substituent hydrogens that are at a distance less than double the H van der Waals radius of 1.2 Å.

reaction is between methoxy radical 4 and ethane A, while the most hindered reaction is between *tert*-butoxy radical 4 with neopentane D. Similarly, for secondary alkane C—H bonds, the least hindered reaction is between 1 and E and the most hindered reaction is between 4 and H; for tertiary alkane C—H bonds, the least hindered reaction is between 1 and I and the most hindered reaction is between 4 and L. Table 7 compares

Table 7. Reaction Enthalpies (Row 1) and Barrier Heights (Row 2) for Least Hindered and Most Hindered HAT Reactions between Alkoxy Radicals and Primary, Secondary, and Tertiary Alkane C-H Bonds (kcal/mol)

	primary C–H (A,1) to (D,4)	secondary C–H (E,1) to (H,4)	tertiary C–H (I,1) to (L,4)
$\Delta \Delta H$	-0.5	-1.2	-2.0
$\Delta\Delta H^{\ddagger}$	-2.5	-2.8	-2.2

the relative barrier heights and relative reaction enthalpies between these least hindered and most hindered HAT reactions for primary, secondary, and tertiary C—H bonds.

For primary, secondary, and tertiary C–H bonds, both the reaction enthalpy and the barrier heights decrease when the alkane reactants go from unhindered to bulky. Presumably, the decrease in reaction enthalpy ΔH is caused by increased hyperconjugative stabilization of the product alkyl radical when the alkane is bulkier. However, the even greater decrease in the barrier heights, ΔH^{\ddagger} , suggests the presence of stabilizing dispersion interactions between the two bulky reactants in the transition state, a finding which we hope encourages further experimental studies. The origins of these dispersion factors are shown graphically in Figure 6. Here, the transition state for the reaction of 4 with C is shown, with the shortest distances between hydrogens on the two reactants labeled. These distances between hydrogens are approximately the sum of the van der Waals radii of two Hs (2.4 Å); that is, the hydrogens

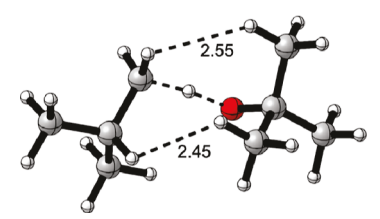


Figure 6. Transition state for the reaction of **4** with **C**, with distances between the nearest hydrogens on the two reactants labeled. These pairs of Hs are just touching, presumably attracting.

are just touching where van der Waals (dispersion) attraction is largest.

4.5. Fitting Sterically Hindered HAT Reactions into Earlier Evans—Polanyi and Roberts—Steel Relationships. We have shown that some steric effects in HAT reactions influence both ΔH and ΔH^{\ddagger} in such a way that the Evans—Polanyi relationship continues to hold. We have also shown small but significant steric repulsion and attraction in several cases. Here, we explicitly test how well the 120 HAT reactions studied in this work fit on the Evans—Polanyi relationship reported by Liu et al. for 104 HAT reactions with alkoxy radicals that differ in their electronegativities. We also consider how these 120 HAT reactions fit into the more general Roberts—Steel relationship also reported by Liu et al. 15

Figure 7 shows the Evans–Polanyi plot from Liu et al. ¹⁵ with the addition of all 120 HAT reactions computed in this work. While the methoxy and *tert*-butoxy radicals were included in the Liu et al. paper, the phenoxy and cyclohexoxy radicals, along with their bulky derivatives, were not. As the figure shows, the new reactions studied in this work fit well onto the Evans–Polanyi plot. In particular, the most sterically hindered radicals studied in this work (6, 8, and 10) fit well into the linear relationship previously established by Liu et al. ¹⁵ for HAT reactions in which there is no α -unsaturation present relative to the reacting C–H bond.

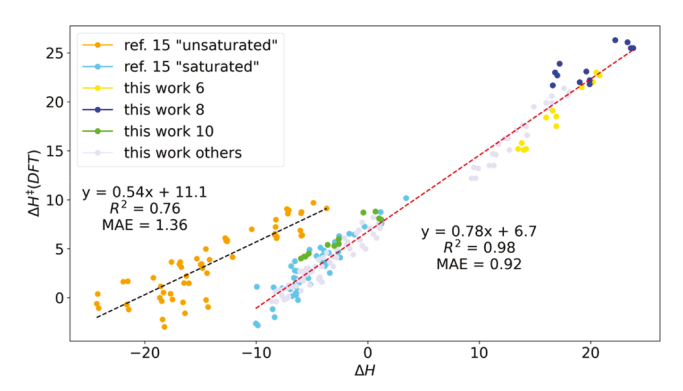


Figure 7. Evans–Polanyi relationship for 104 HAT reactions from Liu et al. 15 with the addition of the 120 HAT reactions studied in this work. The 104 HAT reactions in ref 15 are still classified into "unsaturated" (containing the C–H directly adjacent to the –C=C–, –C=O, –CN, or benzene ring) and "saturated" C–H. They are shown in orange (ref 15 "unsaturated") and light blue (ref 15 "saturated"), respectively. The 120 HAT reactions in this work are all "saturated" C–H. The black and red dashed lines represent linear fits for all "unsaturated" C–H and "saturated" C–H, respectively. The most sterically hindered radicals studied in this work are highlighted on the plot (6 in yellow, 8 in dark blue, and 10 in green) and fit well with the previously studied HAT reactions in which there is no α-unsaturation present relative to the reacting C–H bond (light blue). Enthalpies of activation and enthalpies of reaction are both in kcal/mol.

Because not all of their original 104 HAT reactions could be captured by a single linear Evans–Polanyi relationship, Liu et al. 15 also developed a more general modified Roberts–Steel relationship

$$\Delta H^{\ddagger} = 0.52(1 - d)\Delta H - 0.35\Delta \chi^2 + 10.0 \tag{6}$$

which explicitly accounts for the electronegativity difference $\Delta \chi$ between the two radicals in a HAT reaction as well as whether there is α -unsaturation present relative to the reacting C–H bond (d=0.44) or not (d=0). Thus, we tested how well the 120 HAT reactions studied in this work fit on this modified Roberts–Steel relationship in eq 6; note that d=0 for all reactions in this work because none of the alkane substrates in Figure 3 have any unsaturation.

Figure 8 shows the original Roberts–Steel plot from Liu et al. 15 with the addition of all 120 HAT reactions studied in this work. The *y*-axis is the ΔH^{\ddagger} value computed from eq 6, while the *x*-axis is the ΔH^{\ddagger} value obtained directly from density functional theory (DFT) computations. As the figure shows, the 120 HAT reactions studied in this work fit quite well onto the modified Roberts–Steel plot. As with the Evans–Polanyi plot (Figure 7) discussed previously, the new reactions fit in part because steric effects influence both activation barriers and reaction enthalpies in such a way that the relationship is generally well-preserved. The steric repulsions and attractions we found in this work are also small enough (~1 kcal/mol) to not alter the relationships much.

Finally, we develop a new Roberts-Steel relationship combining the 120 HAT reactions studied in this work with the 104 HAT reactions from Liu et al. 15 studied previously. This refitting including the old data and the data in this work give the equation

$$\Delta H^{\ddagger} = 0.65(1 - d)\Delta H - 0.24\Delta \chi^2 + 9.1 \tag{7}$$

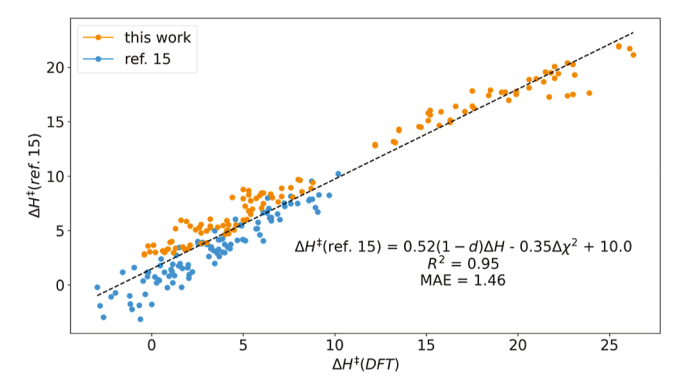


Figure 8. Plot of ΔH^\ddagger obtained via the modified Roberts–Steel relationship in eq 6 from ref 15 vs ΔH^\ddagger obtained from DFT calculations. The 120 HAT reactions studied in this work are shown in blue, while the 104 HAT reactions studied in ref 15 are shown in orange. The dark line is a linear fit of all points, and this line is given by ΔH^\ddagger (ref 15) = $0.83\Delta H^\ddagger$ (DFT) + 1.5, with an R^2 of 0.95 and an MAE of 1.46 kcal/mol. Enthalpies of activation on both axes are in kcal/mol.

where d = 0.44 if there is α -unsaturation present relative to the reacting C-H bond and d = 0 if not (as in all of the 120 HAT reactions studied in this work). Figure 9 is a plot of the ΔH^{\ddagger}

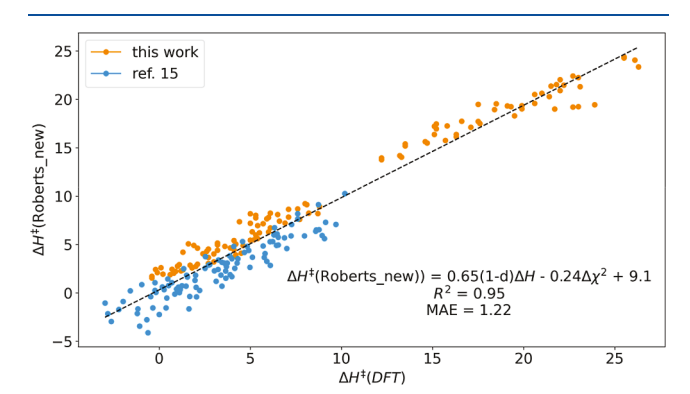


Figure 9. Plot of ΔH^{\ddagger} obtained via the new Roberts–Steel relationship in eq 7 vs ΔH^{\ddagger} obtained from DFT calculations. The Roberts–Steel relationship in eq 7 is explicitly fit to the 120 HAT reactions studied in this work plus the 104 HAT reactions studied in ref 15. Activation enthalpies are given in kcal/mol.

value computed from eq 7 vs the ΔH^{\ddagger} value obtained directly from DFT computations for all 120 HAT reactions studied in this work and all 104 HAT reactions studied previously. As the figure shows, all of these reactions-whether or not the substrates or radicals are sterically hindered—are generally well-accommodated by the single Roberts-Steel relationship in eq 7 with an α value of 0.65, which is slightly higher than the slope of 0.5 found in Marcus theory. The negative β value for $\Delta \chi^2$ (-0.24) is consistent with polarity-matching effects, meaning that as the difference in electronegativity increases, the activation barrier tends to decrease. Although there is no quantitative introduction of steric effects, steric effects are implicitly taken into account through the fine adjustment of the coefficients in front of ΔH^{\ddagger} and $\Delta \chi^2$. Note that all data needed to construct the Evans-Polanyi (Figure 7) and Roberts-Steel (Figures 8 and 9) plots are given in Table S7 in the Supporting Information.

5. CONCLUSIONS

We explored the role of steric effects in HAT reactions by analyzing 120 HAT reactions with both sterically hindered and unhindered radicals and alkane C-H bonds. Because steric repulsion effects may appear not only in the transition states but also in the products, we find that the Evans-Polanyi relationship is generally maintained in HAT reactions between sterically hindered molecules. Activation barriers and reaction enthalpies are both influenced by bulky substituents on the radical but less so by substituents on the alkane. We show that the Evans-Polanyi and modified Roberts-Steel relationships developed for the 104 previously reported HAT reactions are only slightly modified by the inclusion of hindered reactions.

ASSOCIATED CONTENT

Data Availability Statement

The data underlying this study are available in the published article and its Supporting Information.

Supporting Information

The Supporting Information is available free of charge at https://pubs.acs.org/doi/10.1021/acs.joc.3c01361.

Cartesian coordinates of all the structures as well as their computed thermodynamic enthalpies at room temperature, computed electronegativities of radicals used in the simplified Roberts—Steel plots, and all data needed to construct the Evans—Polanyi and Roberts—Steel plots (PDF)

AUTHOR INFORMATION

Corresponding Author

K. N. Houk – Department of Chemistry and Biochemistry, University of California, Los Angeles, California 90095-1569, United States; orcid.org/0000-0002-8387-5261; Email: houk@chem.ucla.edu

Authors

Yi Sun – Yusuf Hamied Department of Chemistry, University of Cambridge, Cambridge CB21EW, England

Fengjiao Liu — College of Chemistry and Chemical Engineering, Shanghai University of Engineering Science, Shanghai 201620, China; ⊚ orcid.org/0000-0002-2039-4786

Jacob N. Sanders — Department of Chemistry and Biochemistry, University of California, Los Angeles, California 90095-1569, United States; oocid.org/0000-0002-2196-4234

Complete contact information is available at: https://pubs.acs.org/10.1021/acs.joc.3c01361

Notes

The authors declare no competing financial interest.

ACKNOWLEDGMENTS

We thank Huiling Shao for helpful discussions. K.N.H. acknowledges the support of the National Science Foundation under award number CHE-2153972. F.L. acknowledges the support of the Shanghai Sailing Program (no. 20YF1416000). Computational resources were provided by the Universities of Cambridge, UCLA, and Shanghai UES.

REFERENCES

- (1) Zhang, C.; Chen, S.; Ye, C.; Harms, K.; Zhang, L.; Houk, K. N.; Meggers, E. Asymmetric Photocatalysis by Intramolecular Hydrogen-Atom Transfer in Photoexcited Catalyst–Substrate Complex. *Angew. Chem., Int. Ed.* **2019**, 58, 14462–14466.
- (2) Deng, Y.; Nguyen, M. D.; Zou, Y.; Houk, K. N.; Smith, A. B. Generation of Dithianyl and Dioxolanyl Radicals Using Photoredox Catalysis: Application in the Total Synthesis of the Danshenspiroketallactones via Radical Relay Chemistry. *Org. Lett.* **2019**, *21*, 1708–1712.
- (3) Cao, H.; Tang, X.; Tang, H.; Yuan, Y.; Wu, J. Photoinduced Intermolecular Hydrogen Atom Transfer Reactions in Organic Synthesis. *Chem Catal.* **2021**, *1*, 523–598.
- (4) Nikolaienko, P.; Jentsch, M.; Kale, A. P.; Cai, Y.; Rueping, M. Electrochemical and Scalable Dehydrogenative C(sp³)–H Amination via Remote Hydrogen Atom Transfer in Batch and Continuous Flow. *Chem.—Eur. J.* **2019**, *25*, 7177–7184.
- (5) Milan, M.; Salamone, M.; Costas, M.; Bietti, M. The Quest for Selectivity in Hydrogen Atom Transfer Based Aliphatic C-H Bond Oxygenation. *Acc. Chem. Res.* **2018**, *51*, 1984–1995.
- (6) Sacramento, J. J. D.; Goldberg, D. P. Factors Affecting Hydrogen Atom Transfer Reactivity of Metal—Oxo Porphyrinoid Complexes. *Acc. Chem. Res.* **2018**, *51*, 2641–2652.
- (7) Shevick, S. L.; Wilson, C. V.; Kotesova, S.; Kim, D.; Holland, P. L.; Shenvi, R. A. Catalytic Hydrogen Atom Transfer to Alkenes: A Roadmap for Metal Hydrides and Radicals. *Chem. Sci.* **2020**, *11*, 12401–12422.
- (8) Wu, J.; Ma, Z. Metal-Hydride Hydrogen Atom Transfer (MHAT) Reactions in Natural Product Synthesis. *Org. Chem. Front.* **2021**, *8*, 7050–7076.
- (9) Zou, L.; Paton, R. S.; Eschenmoser, A.; Newhouse, T. R.; Baran, P. S.; Houk, K. N. Enhanced Reactivity in Dioxirane C—H Oxidations via Strain Release: A Computational and Experimental Study. *J. Org. Chem.* **2013**, *78*, 4037–4048.
- (10) Houk, K.; White, M.; Bigi, M.; Liu, P.; Zou, L. Cafestol to Tricalysiolide B and Oxidized Analogues: Biosynthetic and Derivatization Studies Using Non-Heme Iron Catalyst Fe(PDP). *Synlett* **2012**, 23, 2768–2772.
- (11) Martin, T.; Galeotti, M.; Salamone, M.; Liu, F.; Yu, Y.; Duan, M.; Houk, K. N.; Bietti, M. Deciphering Reactivity and Selectivity Patterns in Aliphatic C–H Bond Oxygenation of Cyclopentane and Cyclohexane Derivatives. *J. Org. Chem.* **2021**, *86*, 9925–9937.
- (12) Bell, R. P. The Theory of Reactions Involving Proton Transfers. *Proc. R. Soc. A* **1936**, *154*, 414–429.
- (13) Evans, M. G.; Polanyi, M. On the Introduction of Thermodynamic Variables into Reaction Kinetics. *Trans. Faraday Soc.* 1937, 33, 448.
- (14) Roberts, B. P.; Steel, A. J. An Extended Form of the Evans—Polanyi Equation: A Simple Empirical Relationship for the Prediction of Activation Energies for Hydrogen-Atom Transfer Reactions. *J. Chem. Soc., Perkin Trans.* 2 **1994**, *10*, 2155—2162.
- (15) Liu, F.; Ma, S.; Lu, Z.; Nangia, A.; Duan, M.; Yu, Y.; Xu, G.; Mei, Y.; Bietti, M.; Houk, K. N. Hydrogen Abstraction by Alkoxyl Radicals: Computational Studies of Thermodynamic and Polarity Effects on Reactivities and Selectivities. *J. Am. Chem. Soc.* **2022**, *144*, 6802–6812.
- (16) Zavitsas, A. A. Hydrogen Abstractions by Radicals. Different Approaches to Understanding Factors Controlling Reactivity. *J. Chem. Soc., Perkin Trans.* 2 **1998**, 3, 499–502.
- (17) Mayer, J. M. Understanding Hydrogen Atom Transfer: From Bond Strengths to Marcus Theory. Acc. Chem. Res. 2011, 44, 36–46.
- (18) Yang, L.-C.; Li, X.; Zhang, S.-Q.; Hong, X. Machine Learning Prediction of Hydrogen Atom Transfer Reactivity in Photoredox-Mediated C–H Functionalization. *Org. Chem. Front.* **2021**, *8*, 6187–6195.
- (19) Wagner, J. P.; Schreiner, P. R. London Dispersion in Molecular Chemistry-Reconsidering Steric Effects. *Angew. Chem., Int. Ed.* **2015**, 54, 12274–12296.

- (20) Tolman, C. A. Steric Effects of Phosphorus Ligands in Organometallic Chemistry and Homogeneous Catalysis. *Chem. Rev.* 1977, 77, 313–348.
- (21) Crossley, M. J.; Field, L. D.; Forster, A. J.; Harding, M. M.; Sternhell, S. Steric Effects on Atropisomerism in Tetraarylporphyrins. *J. Am. Chem. Soc.* **1987**, *109*, 341–348.
- (22) Li, B.; Xu, H.; Dang, Y.; Houk, K. N. Dispersion and Steric Effects on Enantio-/Diastereoselectivities in Synergistic Dual Transition-Metal Catalysis. J. Am. Chem. Soc. 2022, 144, 1971–1985.
- (23) Stable Radicals. In Fundamentals and Applied Aspects of Odd-Electron Compounds; Hicks, R. G., Ed.; John Wiley & Sons, 2010.
- (24) Power, P. P. Persistent and Stable Radicals of the Heavier Main Group Elements and Related Species. *Chem. Rev.* **2003**, *103*, 789–810.
- (25) Francl, M. M.; Pietro, W. J.; Hehre, W. J.; Binkley, J. S.; Gordon, M. S.; DeFrees, D. J.; Pople, J. A. Self-consistent Molecular Orbital Methods. XXIII. A Polarization-type Basis Set for Second-row Elements. *J. Chem. Phys.* **1982**, *77*, 3654–3665.
- (26) Hariharan, P. C.; Pople, J. A. The Influence of Polarization Functions on Molecular Orbital Hydrogenation Energies. *Theor. Chim. Acta* 1973, 28, 213–222.
- (27) Chai, J.-D.; Head-Gordon, M. Long-Range Corrected Hybrid Density Functionals with Damped Atom—Atom Dispersion Corrections. *Phys. Chem. Chem. Phys.* **2008**, *10*, 6615.
- (28) Chai, J.-D.; Head-Gordon, M. Systematic Optimization of Long-Range Corrected Hybrid Density Functionals. *J. Chem. Phys.* **2008**, *128*, 084106.
- (29) Frisch, M. J.; Trucks, G. W.; Schlegel, H. B.; Scuseria, G. E.; Robb, M. A.; Cheeseman, J. R.; Scalmani, G.; Barone, V.; Petersson, G. A.; Nakatsuji, H.; Li, X.; Caricato, M.; Marenich, A. V.; Bloino, J.; Janesko, B. G.; Gomperts, R.; Mennucci, B.; Hratchian, H. P.; Ortiz, J. V.; Izmaylov, A. F.; Sonnenberg, J. L.; Williams; Ding, F.; Lipparini, F.; Egidi, F.; Goings, J.; Peng, B.; Petrone, A.; Henderson, T.; Ranasinghe, D.; Zakrzewski, V. G.; Gao, J.; Rega, N.; Zheng, G.; Liang, W.; Hada, M.; Ehara, M.; Toyota, K.; Fukuda, R.; Hasegawa, J.; Ishida, M.; Nakajima, T.; Honda, Y.; Kitao, O.; Nakai, H.; Vreven, T.; Throssell, K.; Montgomery, J. A., Jr.; Peralta, J. E.; Ogliaro, F.; Bearpark, M. J.; Heyd, J. J.; Brothers, E. N.; Kudin, K. N.; Staroverov, V. N.; Keith, T. A.; Kobayashi, R.; Normand, J.; Raghavachari, K.; Rendell, A. P.; Burant, J. C.; Iyengar, S. S.; Tomasi, J.; Cossi, M.; Millam, J. M.; Klene, M.; Adamo, C.; Cammi, R.; Ochterski, J. W.; Martin, R. L.; Morokuma, K.; Farkas, O.; Foresman, J. B.; Fox, D. J. Gaussian 16, revision C.01.; Gaussian Inc.: Wallingford, CT 2016.
- (30) Beckwith, A. L. J.; Hay, B. P. Kinetics and Mechanism of the Exo Cyclizations of ω -Formylalkyl Radicals. *J. Am. Chem. Soc.* **1989**, 111, 2674–2681.